Asian Journal of Chemistry; Vol. 38, No. 11 (2026), 2993-3001
ASIAN JOURNAL OF CHEMISTRY
https://doi.org/10.14233/ajchem.2026.36700

Natural PTP1B and α-Glucosidase Inhibitors from *Erythrina variegata*: Isolation, Biological Evaluation and Molecular Modelling

NGOC THAO VY TRINH[1,2], THI THUY DO[3], PHI HUNG NGUYEN[3,*], MINH QUAN PHAM[3], THI THUY HUONG LE[3], PHU CHI HIEU TRUONG[4], LE MINH HOANG[5], THI VIET HOA TRUONG[5], DAO CUONG TO[5] and NIEN VINH LAM[1,*]

[1]University of Medicine and Pharmacy, 217 Hong Bang, Ho Chi Minh City 72714, Vietnam
[2]Faculty of Medicine and Pharmacy, Tay Nguyen University, 567 Le Duan, Ea Kao, Dak Lak 630000, Vietnam
[3]Institute of Chemistry, Vietnam Academy of Science and Technology, 18 Hoang Quoc Viet, Nghia Do, Hanoi 122100, Vietnam
[4]School of Medicine and Pharmacy, The University of Danang, Hoa Quy, Ngu Hanh Son, Da Nang city 550000, Vietnam
[5]Phenikaa University Nano Institute, Phenikaa School of Engineering, Phenikaa University, Nguyen Trac, Duong Noi, Hanoi 12116, Vietnam

*Corresponding authors: E-mail: nien@ump.edu.vn; nguyenphihung@ich.vast.vn

Received: 11 August 2026 *Accepted*: 8 October 2026 *Published online*: 13 November 2026 AJC-22530

Erythrina variegata L. has long been used in traditional medicine; however, compound-specific enzyme inhibitory data for constituents of *E. variegata* remain limited. In present study, the phytochemical investigation of the stems of *E. variegata* yielded two known isoflavonoids, erythribyssin H (**1**) and eryvarin R (**2**), which were evaluated for their *in vitro* inhibitory activities against protein tyrosine phosphatase 1B (PTP1B) and α-glucosidase. Compounds **1** and **2** exhibited inhibitory activity against PTP1B with IC_{50} values of 4.12 ± 0.99 and 4.36 ± 0.74 μM, respectively. In the α-glucosidase assay, compounds **1** and **2** showed IC_{50} values of 96.33 ± 0.29 and 101.09 ± 0.87 μM, respectively. Exploratory molecular docking was performed to examine possible interactions with the selected enzyme structures, while absorption, distribution, metabolism, excretion and toxicity (ADMET) predictions provided preliminary estimates of physico-chemical, pharmacokinetic and toxicity-related properties. These findings provide compound-specific *in vitro* evidence of enzyme inhibition by two known constituents of *E. variegata*.

Keywords: *Erythrina variegata* L., Enzyme inhibition, PTP1B inhibition, α-Glucosidase, Molecular docking.

INTRODUCTION

Erythrina variegata L. belongs to the Fabaceae family, the plant grows naturally in lowland mountainous areas and is commonly cultivated as a hedge plant in fields and home gardens in Vietnam [1,2]. In Vietnamese traditional medicine, *E. variegata* has long been used in for various therapeutic purposes. Its leaves are commonly consumed and after heating, applied externally to treat hemorrhoids. In folk medicine, combinations of *E. variegata* leaves with lotus leaves are employed to treat nosebleeds, bloody stools and infantile diarrhea. Furthermore, crushed leaves mixed with potassium permanganate and cold rice are traditionally applied to ulcerative wounds when conventional treatments are ineffective [3]. In Chinese traditional medicine, the bark of *E. variegata* has been extensively used as an antipyretic, antiseptic, diuretic, sedative and sleep-promoting agent. It has also been utilized in the treatment of amoebiasis, diarrhea, amebic dysentery and intestinal parasitic infections [4-6]. The bark has additionally been used to relieve back pain, toothache, paralysis and pruritic skin lesions [5,6].

The phytochemical investigations have revealed that *E. variegata* contains a diverse range of secondary metabolites, including alkaloids, flavonoids, pterocarpans, triterpenes and steroids [3,7-11]. Among the phytochemical constituents, flavonoids, particularly isoflavonoids, have been identified as the major bioactive compounds of this species [12]. Numerous flavonoids have been isolated from *E. variegata* [13-18] such as prenylated isoflavones, flavan-3-ols and coumestane [19-21]. In addition, several isolated triterpenes have also been reported [22,23]. Due to its rich phytochemical profile, *E. variegata* has attracted considerable attention for its diverse biological activities. Previous studies have demonstrated its potential in preventing dental caries, exerting antibacterial effects [6,24],

This is an open access journal, and articles are distributed under the terms of the Attribution 4.0 International (CC BY 4.0) License. This license lets others distribute, remix, tweak, and build upon your work, even commercially, as long as they credit the author for the original creation. You must give appropriate credit, provide a link to the license, and indicate if changes were made.

antioxidant activity [6], analgesic and anti-inflammatory effects [25-27], cardiovascular protection [28] and central nervous system related activities [29-33]. The present study evaluates the *in vitro* inhibitory activities of two known compounds *viz*. erythribyssin H (**1**) and eryvarin R (**2**) against protein tyrosine phosphatase 1B (PTP1B) and α-glucosidase. Erythribyssin H has previously been isolated from *E. abyssinica* [34], whereas eryvarin R has been reported from *E. variegata* [35]. The study reports the experimental evaluation of two known compounds isolated from *E. variegata* against both enzymes. Molecular docking and ADMET predictions were used to assess potential protein–ligand interactions, physico-chemical and safety limitations.

EXPERIMENTAL

The stem of *Erythrina variegata* L. was collected from the local garden in Hanoi, Vietnam. A voucher specimen (VN01HN) was deposited at the Department of Chemical Analysis, Institute of Chemistry, Vietnam Academy of Science and Technology (VAST). The NMR spectral data were measured on a spectrometer AVANCE 500 series of Bruker. Silica gel normal phase and reverse phase were procured from Merck Chemicals Ltd. Thin layer chromatography (TLC) was performed using both silica gel NP and RP F_{254} plates. An Agilent 1260 HPLC (high-performance liquid chromatography) system was used for isolation and purification purpose with an RP-C18 column (10 × 250 mm, 5 μm particle size). Acetonitrile and methanol were purchased from Fisher Scientific Korea Ltd. for HPLC purification, whereas DMSO was purchased for use as the solvent in the enzyme-inhibition assays.

Isolation of compounds: The stems of *E. variegata* were cleaned to remove impurities, finely chopped, thoroughly washed and dried at approximately 50 ºC until the moisture content reached about 10%. The dried material was ground to a particle size of ~2.0 mm, yielding 2.0 kg of stem powder. The powder was extracted three times with *n*-hexane using a 1:3 (w/v) ratio in an ultrasonic apparatus at 35 ºC for 90 min per extraction. After separation of the solvent, the residual plant material was extracted with EtOAc at a 1:5 (w/v) ratio using the same apparatus at 40 ºC for 120 min. The extract was filtered and concentrated by vacuum distillation to obtain 130 g of crude EtOAc extract.

The crude extract was subjected to normal-phase silica gel column chromatography using silica gel with a particle size of 63-200 μm. Elution was performed with an *n*-hexane/acetone solvent system, with the ratio gradually changed from 10:1 to 1:10 (v/v), yielding 13 fractions (EV.F1–EV.F13). Fraction EV.F11 was further separated using an RP-C18 column (5.0 × 60 cm; particle size, 150 μm) with a stepwise MeOH–H_2O gradient ranging from 1:5 to 5:1 (v/v), yielding ten subfractions (F11-1–F11-10). Subfraction F11-3 was purified by semi-preparative HPLC using an Agilent 1260 Infinity system with an isocratic mobile phase of 32% MeCN in H_2O over 70 min. This purification yielded compound 1 (11.7 mg, t_R = 55.1 min) and compound 2 (8.9 mg, t_R = 38.5 min).

The isolation procedure was based on chromatographic separation rather than bioassay-guided fractionation. No PTP1B or α-glucosidase inhibition assays were performed on the crude EtOAc extract, fractions EV.F1–EV.F13 or subfractions F11-1–F11-10.

Compound 1: Light brown powder; ^{1}H NMR (500 MHz, acetone-d_6, δ ppm): 4.81 (2H, m, H-2ax/H-2eq), 4.21 (1H, dd, *J* = 4.0, 6.0 Hz, H-3), 6.88 (1H, d, *J* = 8.0 Hz, H-5), 6.37 (1H, dd, *J* = 2.0, 8.0 Hz, H-6), 6.30 (1H, d, *J* = 2.5 Hz, H-8), 6.57 (1H, s, H-3′), 6.58 (1H, s, H-6′), 3.63 (3H, s, 2′-OCH_3), 3.78 (3H, s, 5′-OCH_3); ^{13}C NMR (100 MHz, acetone-d_6, δ ppm): 80.0 (C-2), 41.4 (C-3), 122.0 (C-4), 126.7 (C-5), 108.2 (C-6), 159.4 (C-7), 98.5 (C-8), 163.0 (C-9), 122.8 (C-1′), 153.0 (C-2′), 101.0 (C-3′), 147.5 (C-4′), 142.1 (C-5′), 113.7 (C-6′), 56.3 (2′-OCH_3), 57.1 (5′-OCH_3).

Compound 2: Yellow powder; ^{1}H NMR (500 MHz, acetone-d_6, δ ppm): 9.59 (1H, s, CHO), 5.43 (1H, d, *J* = 9.0 Hz, H-2a), 4.28 (1H, d, *J* = 9.0 Hz, H-2b), 7.13 (1H, d, *J* = 8.0 Hz, H-5), 6.51 (1H, dd, *J* = 1.5, 8.0 Hz, H-6), 6.38 (1H, d, *J* = 1.5 Hz, H-8), 6.65 (1H, s, H-3′), 6.71 (1H, s, H-6′), 3.67 (3H, s, 2′-OCH_3), 3.74 (3H, s, 5′-OCH_3); ^{13}C NMR (100 MHz, acetone-d_6, δ ppm): 79.2 (C-2), 63.7 (C-3), 116.2 (C-4), 127.2 (C-5), 101.3 (C-6), 160.4 (C-7), 98.6 (C-8), 163.2 (C-9), 120.1 (C-1′), 152.5 (C-2′), 108.8 (C-3′), 142.9 (C-4′), 148.9 (C-5′), 114.1 (C-6′), 56.0 (2′-OCH_3), 57.0 (5′-OCH_3), 195.6 (3-CHO).

PTP1B inhibitory assay: The inhibitory activity of compounds isolated from the stems of *E. variegata* against protein tyrosine phosphatase 1B (PTP1B) was evaluated using an *in vitro* enzymatic assay according to a previously described method [36]. The assay is based on the hydrolysis of *p*-nitrophenyl phosphate (*p*-NPP) by PTP1B to produce *p*-nitrophenol, a yellow-coloured product measurable at 405 nm. The amount of *p*-nitrophenol formed is directly proportional to the enzymatic activity of PTP1B. Each reaction well (final volume: 110 μL) contained 2 mM *p*-NPP and 0.05-0.1 μg PTP1B enzyme in assay buffer consisting of 50 mM citrate buffer (pH 6.0), 0.1 M NaCl, 1 mM EDTA and 1 mM dithiothreitol (DTT), in the presence or absence of the test compounds. The vehicle control served as the no-inhibitor control and contained the complete enzyme reaction mixture with 0.5% (v/v) DMSO but no test compound. The same final DMSO concentration was maintained in all test and control wells. Ursolic acid was used as the positive control for the PTP1B assay. The reaction mixture was pre-incubated at 37 ºC for 10 min followed by the addition of 50 μL of *p*-NPP solution prepared in the same buffer. After incubation at 20 ºC for 20 min, the reaction was terminated by adding 10 M NaOH. The absorbance was measured at 405 nm using a spectrophotometer. Background hydrolysis of *p*-NPP in the absence of PTP1B served as the enzyme blank for blank correction. Each assay was performed in three independent assay runs.

α-Glucosidase inhibitory assay: The inhibitory activity against α-glucosidase was evaluated according to a previously reported 96-well microplate method with minor modifications [37]. The final reaction volume was 200 μL per well. The reaction mixture consisted of 2.5 mM *p*-nitrophenyl-α-D-glucopyranoside, 100 mM phosphate buffer (pH 6.8), α-glucosidase enzyme (0.2 U/mL) and test samples (10 μL) at various concentrations. The vehicle/no-inhibitor control contained 0.5% (v/v) DMSO without test compound and the same

final DMSO concentration was maintained in all test and control wells. Acarbose was used as the positive control for the α-glucosidase assay. The reaction mixtures were incubated at 37 ºC for 30 min and the reaction was terminated by the addition of 0.1 M Na_2CO_3. The absorbance was measured at 405 nm using an Infinite F50 spectrophotometer (Tecan, Switzerland). The enzyme blank contained all reaction components except α-glucosidase and contained the same final DMSO concentration. The percentage inhibition of α-glucosidase activity (% inhibition) was calculated using the following equation:

$$\text{Inhibition (\%)} = \frac{A_C - A_T}{A_C - A_O}$$

where % I: Percentage of α-glucosidase enzyme activity inhibited; A_C: Absorbance of the control sample (without test sample); A_T: Absorbance of the test sample; A_O: Absorbance of the enzyme blank, containing the reaction components and 0.5% (v/v) DMSO but no α-glucosidase enzyme. Each assay was performed in three independent assay runs.

Protein preparation: The crystal structures of the target proteins were retrieved from the RCSB Protein Data Bank [38]. Human PTP1B complexed with the catalytic-site ligand TPI (PDB ID: 1BZC) and the allosteric-site ligand FRJ (PDB ID: 1T4J) were used as structural references for catalytic- and allosteric-site docking, respectively. The two structures were aligned to compare their corresponding binding regions. The docking poses and scores were not independently validated experimentally.

For exploratory α-glucosidase docking, the crystal structure of human lysosomal acid α-glucosidase (GAA) complexed with acarbose (PDB ID: 5NN8) was retrieved from the RCSB Protein Data Bank. This structure represents lysosomal GAA, not intestinal brush-border α-glucosidase, which limits the direct relevance of the docking results to intestinal α-glucosidase inhibition. Protein preparation followed a reported protocol [37]. Water molecules and co-crystallized ligands were removed and the structures were energy-minimized using Swiss-PdbViewer [39] with default optimization parameters. Polar hydrogen atoms were added using AutoDockTools version 1.5.6 [40] and the prepared structures were saved in PDBQT format for subsequent docking simulations.

Ligand preparation: The three-dimensional (3D) structures of the isolated compounds were generated using MarvinSketch (ChemAxon, USA). Geometry optimization was subsequently performed using the MMFF94 force field implemented in Avogadro [41]. The co-crystallized reference ligands TPI from PDB ID 1BZC, FRJ from PDB ID 1T4J and acarbose from PDB ID 5NN8 were extracted and prepared using the same procedure as the test compounds for comparative docking. Finally, torsional bonds were assigned using AutoDock Tools version 1.5.6 [40] and all ligands were converted into PDBQT format for molecular docking studies.

Molecular docking simulation: The molecular docking simulations were carried out using AutoDock Vina version 1.1.2 [42]. The binding-site grids were defined based on the coordinates of the corresponding co-crystallized ligands in each protein structure. The resulting AutoDock Vina docking scores were reported in kcal/mol as computational outputs for comparative exploration. The interactions between the ligands and target proteins were visualized and analyzed using BIOVIA Discovery Studio Visualizer 2020.

ADMET prediction: Lipinski's rule of five [43] was used as a descriptive framework to assess the calculated molecular descriptors of compounds 1 and 2. Their physicochemical and pharmacokinetic properties were predicted in silico using SwissADME [44], while acute oral toxicity was estimated separately using the DL-AOT Prediction Server [45]. These computational predictions do not establish drug-likeness, oral bioavailability, safety, or therapeutic suitability.

Statistical analysis: Each assay was conducted in three independent assay runs using purified enzymes; these runs do not represent biological replicates from independent biological samples. Data are expressed as mean ± standard deviation (SD). IC_{50} values were derived from plots of $\log_{10}$ concentration against percentage inhibition. No formal inferential statistical tests or 95% confidence intervals were calculated. Accordingly, *p*-values and confidence intervals are not reported and differences between the test compounds and reference inhibitors are interpreted descriptively rather than as evidence of statistical significance.

RESULTS AND DISCUSSION

Compounds **1** and **2** were purified by a semi-preparative Agilent HPLC 1260 series with an isocratic solvent system of 32% MeCN in H_2O and an RP-C18 column. The ^1H and ^{13}C NMR spectra of **1** and **2** displayed similar spectral patterns with characteristic signals attributed to aromatic protons of two benzene rings, along with those corresponding to hydroxyl groups (C-7 and C-4′) and two methoxy groups (Fig. 1). The ^1H NMR of compound **1** displayed an AMX-type spin system at δ_H 4.80-4.82 (2H, m, H-2ax/H-2eq), 4.21 (1H, dd, J = 4.0, 6.0 Hz, H-3) and its ^{13}C NMR spectrum showed a methylene carbon at C-2 (δ_C 80.0) and a methine carbon at C-3 (δ_C 41.4). This indicated a 3-aryl-2,3-dihydrobenzofuran skeleton for compound **1** [34]. Similarly, the ^{13}C NMR spectrum of compound **2** showed a methylene carbon at C-2 (δ_C 79.2) and a methine carbon at C-3 (δ_C 63.7) and an additional aldehyde group (δ_C 195.6) with corresponding proton signal at δ_H 9.59 (1H, s). However, its ^1H NMR displayed only two proton signals at δ_H 5.43 (1H, d, J = 9.0 Hz) and 4.28 (1H, d, J = 9.0 Hz) for H-2a and H-2b, respectively, but no proton signal for H-3. Comparison of the ^1H- and ^{13}C NMR data of these compounds with references led to the identification of the structures of compound **1** as erythribyssin H [34] and compound **2** as eryvarin R [35]. The PTP1B and α-glucosidase inhibition assays reported below were performed only with the purified compounds erythribyssin H (**1**) and eryvarin R (**2**).

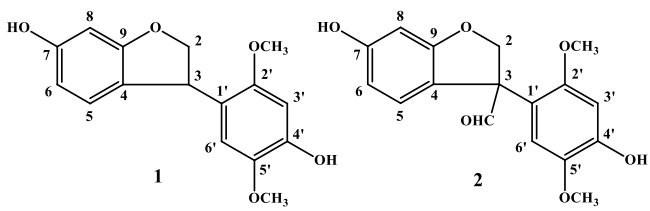


Fig. 1. Chemical structures of compounds **1** and **2** isolated from *E. variegata*

PTP1B inhibitory activity of isolated compounds: Erythribyssin H (**1**) and eryvarin R (**2**) inhibited PTP1B with IC_{50} values of 4.12 ± 0.99 and 4.36 ± 0.74 μM, respectively, whereas the positive control, ursolic acid, exhibited an IC_{50} value of 3.37 ± 0.18 μM under the same assay conditions (Table-1). The results confirm PTP1B inhibition under the conditions of the biochemical assay. The two compounds showed numerically similar IC_{50} values. Although compound **2** contains a formyl group at C-3, the available data are insufficient to determine its effect on inhibitory potency.

TABLE-1
INHIBITORY ACTIVITY DATA OF COMPOUNDS **1** AND **2** AGAINST PTP1B AND α-GLUCOSIDASE

Compounds	PTP1B inhibition (IC_{50}, μM)	α-Glucosidase inhibition (IC_{50}, μM)
Erythribyssin H (**1**)	4.12 ± 0.99	96.33 ± 0.29
Eryvarin R (**2**)	4.36 ± 0.74	101.09 ± 0.87
Ursolic acid[a]	3.37 ± 0.18	–
Acarbose[b]	–	123.54 ± 0.29

[a]Reference compound for PTP1B; [b]Reference compound for α-glucosidase. Values are presented as mean ± SD from three independent assay runs.

α-Glucosidase inhibitory activity: In the α-glucosidase assay, compounds **1** and **2** exhibited IC_{50} values of 96.33 ± 0.29 and 101.09 ± 0.87 μM, respectively, when compared with 123.54 ± 0.29 μM for acarbose (Table-1). Both compounds therefore had numerically lower IC_{50} values than acarbose under the conditions used. The small numerical difference between compounds **1** and **2** is insufficient to establish the contribution of the formyl substituent to inhibition.

For comparison with related flavonoids, prenylated flavonoids isolated from the related species *E. mildbraedii* were reported to inhibit PTP1B with IC_{50} values ranging from 5.3 to 42.6 μM [46]. The IC_{50} values obtained for compounds **1** and **2** (4.12 and 4.36 μM, respectively) were close to or slightly lower than the lower end of this reported range. However, this comparison is tentative since the assay conditions and compound structures were not identical. In a separate structure activity study of flavonoids against yeast α-glucosidase, quercetin and apigenin showed IC_{50} values of 15 and 82 μM, respectively [47]. Under the present assay conditions, compounds **1** and **2** showed IC_{50} values of 96.33 and 101.09 μM.

Molecular docking study: Molecular docking was used to explore predicted poses and interactions of the isolated compounds with selected PTP1B and α-glucosidase structures. PTP1B regulates insulin signaling and is a potential target in metabolic disease research [48]. Its structure contains a conserved, polar catalytic region and an allosteric site approximately 20 Å away, involving helices α3, α6 and α7 [49,50] (Fig. 2). These structural features provided the basis for comparing the predicted interactions of erythribyssin H (**1**) and eryvarin R (**2**), isolated from *E. variegata*, at the two PTP1B reference sites.

The predicted docking scores for compounds **1** and **2** at the catalytic and allosteric sites are shown in Table-2. At the catalytic site, both compounds yielded identical scores of -6.9 kcal/mol, compared with -8.9 kcal/mol for the co-crystallized reference ligand TPI in PDB structure 1BZC. At the allosteric site, the predicted scores were -7.3 and -6.7 kcal/mol for compounds **1** and **2**, respectively, compared with -6.8 kcal/mol for the co-crystallized reference ligand FRJ in PDB structure 1T4J.

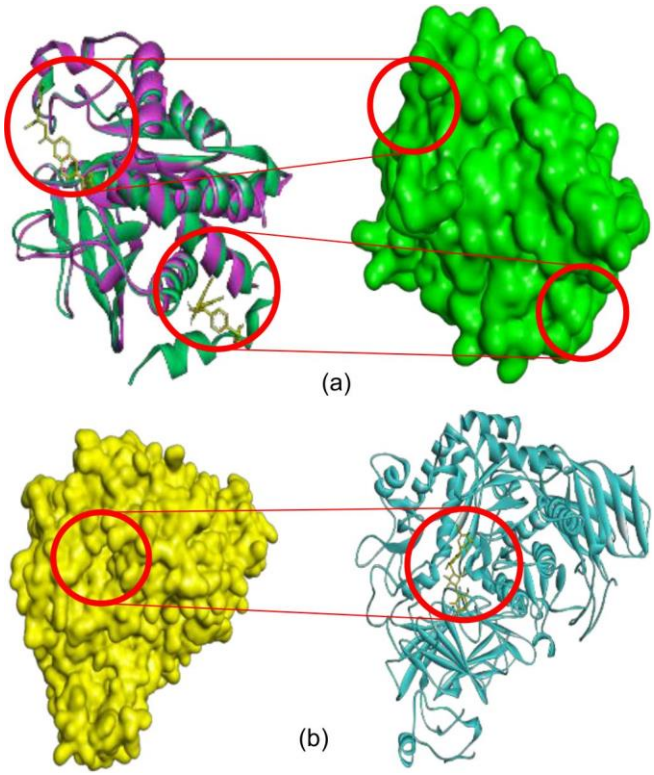


Fig. 2. Structural reference sites used for docking: (a) superposition of the PTP1B crystal structures (PDB IDs 1BZC and 1T4J) with their co-crystallized ligands at the catalytic and allosteric sites, respectively; and (b) human lysosomal acid α-glucosidase (GAA; PDB ID 5NN8) with its co-crystallized acarbose ligand

TABLE-2
MOLECULAR DOCKING SCORES (kcal/mol) OF COMPOUNDS **1** AND **2** AND CO-CRYSTALLIZED REFERENCE LIGANDS

Compound or reference ligand	PTP1B catalytic site (PDB 1BZC)	PTP1B allosteric site (PDB 1T4J)	Human lysosomal acid α-glucosidase/GAA (PDB 5NN8)
1	-6.9	-7.3	-6.6
2	-6.9	-6.7	-7.1
TPI[a]	-8.9	–	–
FRJ[b]	–	-6.8	–
Acarbose[c]	–	–	-6.7

[a]Co-crystallized catalytic-site ligand in PDB ID 1BZC; [b]Co-crystallized allosteric-site ligand in PDB ID 1T4J; [c]Co-crystallized reference ligand in PDB ID 5NN8.

At the catalytic site of PTP1B (PDB ID: 1BZC), the co-crystallized carbamoyl-based butyric acid ligand was reported to form hydrogen-bond contacts involving Gly218, Gly220, Ser216, Ala217, Arg47, Asp48, Cys215 and Ile219, together with hydrophobic contacts involving Arg221, Phe182 and Tyr46. The predicted binding poses of compounds **1** and **2** are shown in Fig. 3. Erythribyssin H (**1**) showed predicted hydrogen bond contacts with Tyr120, Ala159, Gly160 and Ser214, alongside hydrophobic contacts with Ala159, Gly160, Ile162, Asp186

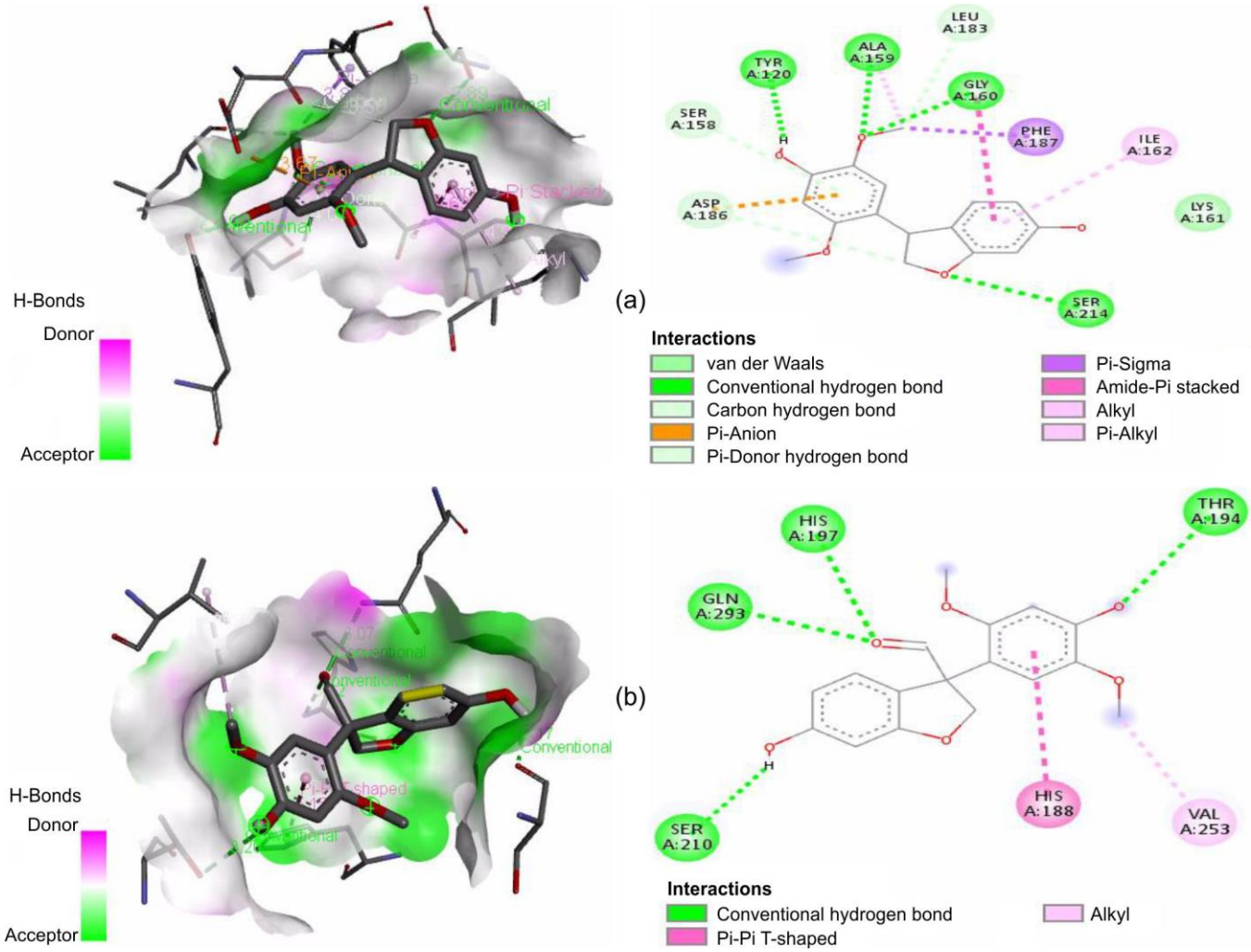


Fig. 3. 2D ligand interaction diagrams and binding modes for PTP1B at the catalytic site: (a) erythribyssin H (**1**) and (b) eryvarin R (**2**)

and Phe187. Eryvarin R (**2**) showed hydrogen-bond contacts with Thr194, His197, Ser210 and Gln293, along with hydrophobic contacts with His188 and Val253.

At the PTP1B allosteric site (PDB ID: 1T4J), the co-crystallized reference ligand formed hydrogen bonds with Arg79, Ser285 and Ile281 and hydrophobic contacts with Glu200, Asp236, Ile281 and Arg199. As shown in Fig. 4a, compound **1** lacked conventional hydrogen bonds and showed hydrophobic contacts with Leu192, Phe196, Phe280 and Ile281. Compound **2** formed no conventional hydrogen bonds, with hydrophobic contacts limited to Phe196 and Phe280.

The α-glucosidase docking study used human lysosomal acid α-glucosidase (GAA; PDB ID: 5NN8) with acarbose as the reference ligand. Compounds **1** and **2** had predicted docking scores of -6.6 and -7.1 kcal/mol, respectively, as compared with -6.7 kcal/mol for acarbose (Table-2). Acarbose was predicted to form hydrogen bonds with Ser676, Ser679, Asp282 and Asp616. Compound **1** showed hydrophobic contacts with Arg608, His717, Leu865 and Val867, without conventional hydrogen bonds. Compound **2** was predicted to form hydrogen bonds with Met363, Glu866 and Glu869, alongside hydrophobic contacts with His717 and Leu868 (Fig. 5). These computational contacts do not confirm actual binding or enzyme inhibition.

Physico-chemical descriptors and Lipinski's rule of five: Lipinski's rule of five [43] was used to assess selected molecular descriptors of compounds **1** and **2**, together with molecular weight, hydrogen-bond donors and acceptors and calculated logP. Both compounds met the criteria without formal violations. SwissADME [44] was used to calculate rotatable bonds, topological polar surface area (TPSA), molar refractivity and predicted aqueous solubility (Table-3). Both compounds had three rotatable bonds, with TPSA values of 68.15 and 85.22 Å^2 and predicted log S values of -3.44 and -3.07, respectively.

***in silico* ADME:** The ADME predictions generated using SwissADME [44] are shown in Table-4. Both compounds were classified by the model as having high predicted gastrointestinal absorption. Compound **1** was predicted to be blood brain barrier (BBB)-permeant, whereas compound **2** was not classified as BBB-permeant. The predicted skin permeability coefficients (log Kp) were -6.21 and -6.94 cm/s for compounds **1** and **2**, respectively, which is consistent with low predicted skin permeability under the applied model.

SwissADME predictions for cytochrome P450 (CYP) inhibition and P-glycoprotein (P-gp) substrate status are shown in Table-4 [44]. Both compounds were predicted to inhibit

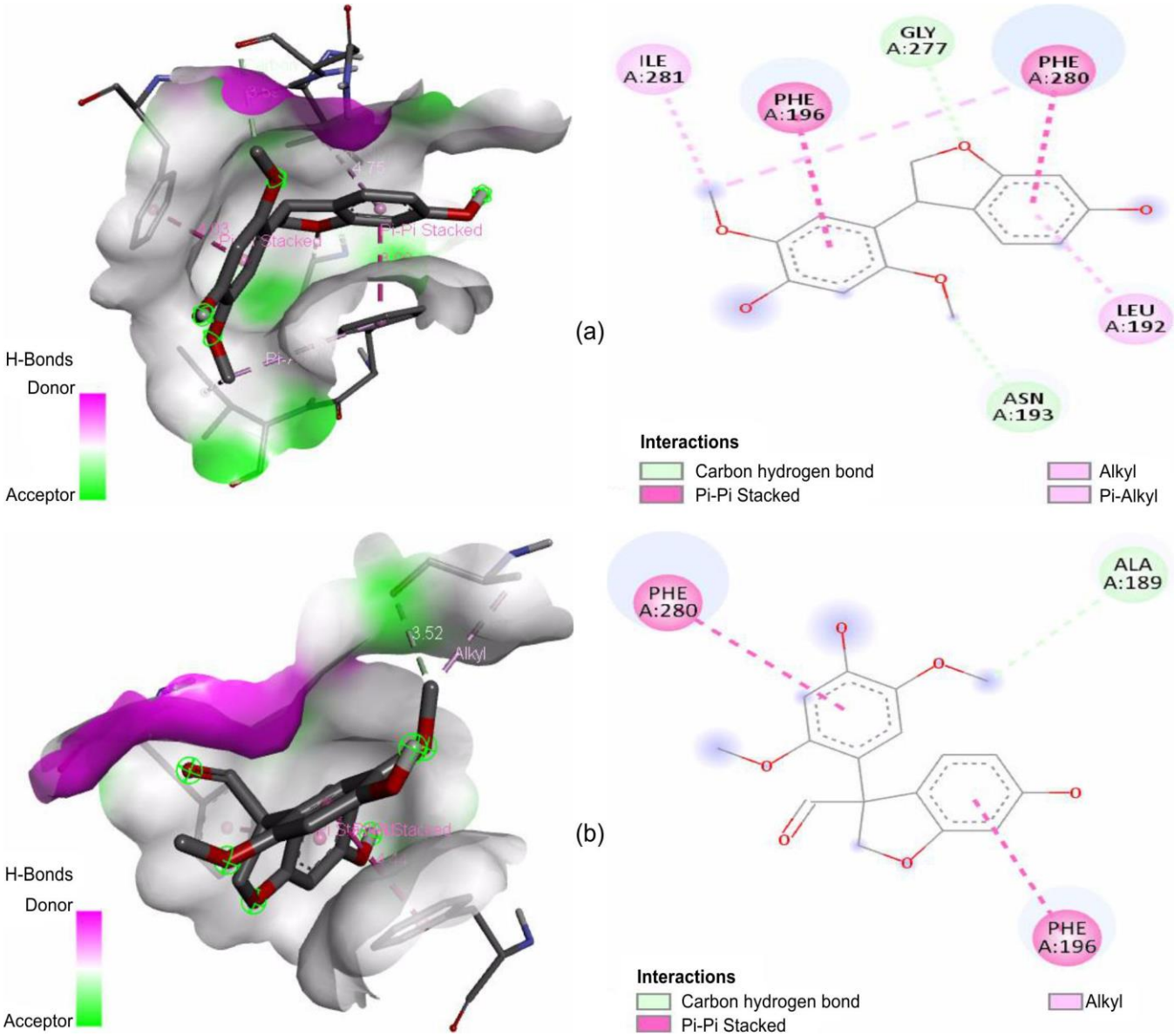


Fig. 4. 2D ligand interaction diagrams and binding modes for PTP1B at the allosteric site: (a) erythribyssin H (**1**) and (b) eryvarin R (**2**)

TABLE-3
PHYSICO-CHEMICAL PROPERTIES AND DRUG-LIKENESS OF COMPOUNDS **1** AND **2**

Compound	MW (g/mol)	Log P	nHBD	nHBA	TPSA	MR	Lipinski violation	Log S	nRotB
1	288.30	2.38	2	5	68.15	77.30	0	–3.44	3
2	316.31	1.86	2	6	85.22	82.19	0	–3.07	3

MW: molecular weight; log P: log of octanol/water partition coefficient; nHBD: number of hydrogen bond donor(s); nHBA: number of hydrogen bond acceptor(s); TPSA: topological polar surface area (Å); MR: molar refractivity; log S: log of solubility; nRotB: number of rotatable bond(s).

TABLE-4
PREDICTED ADME PROPERTIES AND PHARMACOKINETIC PROFILES OF COMPOUNDS **1** AND **2**

Compound	Log K_p (cm/s)	GI Abs	BBB per	Inhibitor interaction					
				P-gp substrate	CYP1A2 Inhibitor	CYP2C19 Inhibitor	CYP2C9 Inhibitor	CYP2D6 Inhibitor	CYP3A4 Inhibitor
1	–6.21	High	Yes	Yes	Yes	No	No	Yes	Yes
2	–6.94	High	No	Yes	Yes	No	No	No	Yes

Log K_p: log of skin permeability; GI Abs: Gastro-intestinal absorption; BBB Per: Blood brain barrier permeability; P-gp: P-glycoprotein; CYP: cytochrome P450.

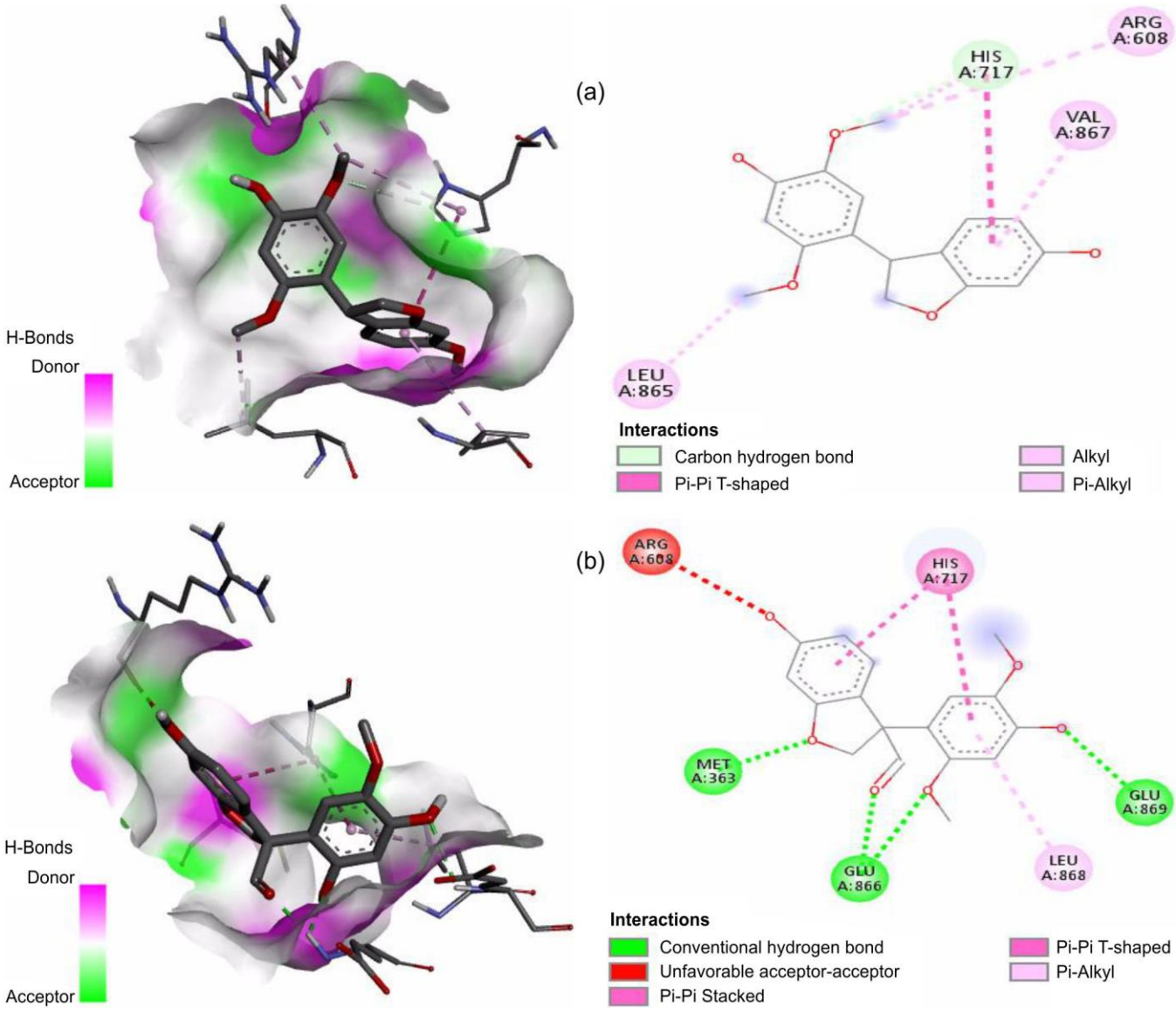


Fig. 5. Predicted ligand interaction diagrams and docking poses for human lysosomal acid α-glucosidase (GAA; PDB ID 5NN8): (a) erythribyssin H (**1**) and (b) eryvarin R (**2**)

CYP1A2 and CYP3A4, with no alerts for CYP2C19 or CYP2C9. Compound **1** generated a CYP2D6 inhibition alert, whereas compound **2** did not. Both were predicted to be P-gp substrates.

Predicted acute oral toxicity: Acute oral toxicity was estimated using the DL-AOT Prediction Server [45]. The predicted LD_{50} values were found to be 3.05 and 2.80 mg/kg for compounds **1** and **2**, respectively, and both compounds were assigned to the "Caution" category (Table-5).

The SwissADME radar plots summarize the predicted physicochemical profiles of erythribyssin H (**1**) and eryvarin R (**2**) relative to model-defined ranges for lipophilicity, size, polarity, solubility, flexibility and saturation (Fig. 6) [44]. Both compounds showed deviations in INSATU and compound **2** exhibited higher deviations in polarity- and solubility-related descriptors. These results describe calculated molecular properties rather than experimentally verified pharmacokinetic behaviour.

TABLE-5
TOXICITY OF COMPOUNDS **1** AND **2** FROM *E. variegata* PREDICTED USING DL-AOT PREDICTION SERVER

Compound	LD_{50} (mg/kg)	Toxicity
1	3.05	Caution
2	2.80	Caution

LD_{50}, predicted median lethal dose (mg/kg); DL-AOT, deep-learning-based acute oral toxicity prediction server. The LD_{50} values and toxicity categories are *in silico* predictions generated by the server and do not represent experimentally measured toxicity or establish safety. "Caution" denotes the classification assigned by the prediction server.

Conclusion

Two known isoflavonoids, erythribyssin H (**1**) and eryvarin R (**2**), were isolated from the stems of *Erythrina variegata* and identified by ^{1}H and ^{13}C NMR data. Both compounds exhibited *in vitro* PTP1B inhibitory activity, with IC_{50} values

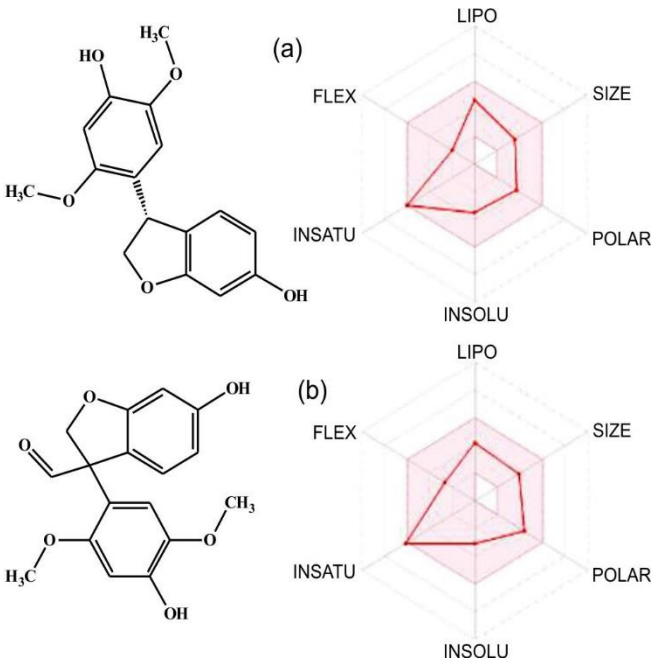


Fig. 6. Bioavailability radar for compounds **1** and **2**

of 4.12 ± 0.99 and 4.36 ± 0.74 μM, respectively and α-glucosidase inhibitory activity, with IC_{50} values of 96.33 ± 0.29 and 101.09 ± 0.87 μM. Molecular docking provided predicted interaction profiles at the catalytic and allosteric sites of PTP1B and with human lysosomal acid α-glucosidase. Swiss-ADME analysis characterized their predicted physicochemical and pharmacokinetic properties, while the DL-AOT server provided preliminary acute oral toxicity estimates. The study establishes the enzyme-inhibitory activity of these two isolated compounds under the tested conditions and combines biochemical assays with computational analyses to characterize their interaction profiles and predicted properties.

ACKNOWLEDGEMENTS

This study was financially supported by the Vietnam Academy of Science and Technology, code no. VAST04.02/24-25. The authors thank the Centre for Nuclear Magnetic Resonance, Institute of Chemistry, Vietnam Academy of Science and Technology, for recording the NMR spectra.

CONFLICT OF INTEREST

The authors declare that there is no conflicts of interest regarding the publication of this article.

DECLARATION OF AI-ASSISTED TECHNOLOGIES

During the preparation of this manuscript, the authors used an AI-assisted tool(s) to improve the language and no data, results or scientific conclusions were generated by AI. All analyses, interpretations and conclusions are the authors' own. The authors reviewed and edited the content and take full responsibility for the published work.

REFERENCES

1. A. Kumar, S. Lingadurai, A. Jain and N.R. Barman, *Pharmacogn. Rev.*, **4**, 147 (2010); https://doi.org/10.4103/0973-7847.70908
2. E. Susilawati, J. Levita, Y. Susilawati and S.A. Sumiwi, *Front. Pharmacol.*, **14**, 1281150 (2023); https://doi.org/10.3389/fphar.2023.1281150
3. P.-H. Nguyen, N.-T.-V. Trinh, T.-T. Do, T.-H. Vu, D.C. To, H.K.T. Pham, P.C.H. Truong, K.T.P. Van and M.H. Tran, *J. Chem. Res.*, **48**, 1 (2024); https://doi.org/10.1177/17475198231226382
4. M. Anwar, Ph.D. Thesis, The Pharmacognostic and Pharmacological Studies on Medicinal Valued Herbal Drugs, *Erythrina variegata var. orientalis*, *Matricaria chamomilla*, *Psoralea corylifolia* and *Chenopodium album*, Faculty of Pharmacy, University of Karachi, Karachi, Pakistan (2006).
5. S. Karunanithi, V.B. Rajkishore and R. Ramalingam, *Res. J. Pharmacogn. Phytochem.*, **9**, 37 (2017); https://doi.org/10.5958/0975-4385.2017.00006.1
6. S. Kumar, R. Malhotra and D. Kumar, *Pharmacogn. Rev.*, **4**, 58 (2010); https://doi.org/10.4103/0973-7847.65327
7. S. Ghosal, S.K. Dutta and S.K. Bhattacharya, *J. Pharm. Sci.*, **61**, 1274 (1972); https://doi.org/10.1002/jps.2600610821
8. B.J. Zhang, J. Wu, M.F. Bao, F. Wang and X.H. Cai, *Nat. Prod. Bioprospect.*, **10**, 57 (2020); https://doi.org/10.1007/s13659-020-00235-3
9. Y.T. Tang, J. Wu, M.F. Bao, Q.G. Tan and X.H. Cai, *Phytochemistry*, **198**, 113160 (2022); https://doi.org/10.1016/j.phytochem.2022.113160
10. Y.T. Tang, Z.R. Si, M.F. Bao and X.H. Cai, *Fitoterapia*, **166**, 105408 (2023); https://doi.org/10.1016/j.fitote.2022.105408
11. P. Sumi and N. Nirmala Devi, *Res. J. Pharmacogn. Phytochem.*, **15**, 298 (2023); https://doi.org/10.52711/0975-4385.2023.00047
12. V.H. Deshpande, A.D. Pendse and R. Pendse, *Indian J. Chem.*, **15B**, 205 (1977).
13. N.J. Sadgrove, T.B. Oliveira, G.P. Khumalo, S.F. van Vuuren and B.-E. van Wyk, *Antibiotics*, **9**, 223 (2020); https://doi.org/10.3390/antibiotics9050223
14. H. Tanaka, M. Doi, H. Etoh, N. Watanabe, H. Shimizu, M. Hirata, M. Ahmad, I. Qurashi and M.R. Khan, *J. Nat. Prod.*, **64**, 1336 (2001); https://doi.org/10.1021/np0101696
15. Y. Zhang, X.L. Li, X.S. Yao and M.S. Wong, *Arch. Pharm. Res.*, **31**, 1534 (2008); https://doi.org/10.1007/s12272-001-2147-5
16. S. Muthukrishnan, S. Palanisamy, S. Subramanian, S. Selvaraj, K.R. Mari and R. Kuppulingam, *J. Acupunct. Meridian Stud.*, **9**, 207 (2016); https://doi.org/10.1016/j.jams.2016.06.001
17. M.Z. Rahman, M.S. Rahman, A. Kaisar, A. Hossain and M.A. Rashid, *Turk. J. Pharm. Sci.*, **7**, 21 (2010).
18. M.K. Alam, Z.H. Rana, S.N. Islam and M. Akhtaruzzaman, *Food Chem.*, **320**, 126646 (2020); https://doi.org/10.1016/j.foodchem.2020.126646
19. W.Y. Ahmad, I.M. Said, S.Y. Soon, H. Takayama, M. Kitajima and N. Aimi, *Online J. Biol. Sci.*, **2**, 542 (2002); https://doi.org/10.3923/jbs.2002.542.544
20. H. Singh, A.S. Chawla, A.K. Jindal, A.H. Conner and J.W. Rowe, *Lloydia*, **38**, 97 (1975).
21. T.D. Samanta and S. Laskar, *Food Chem.*, **114**, 212 (2009); https://doi.org/10.1016/j.foodchem.2008.09.040
22. T.K. Lim, Edible Medicinal and Non-Medicinal Plants: Flowers, Springer: Dordrecht, vol. 7, pp. 788-805 (2014).
23. F. Tabassum, C.M. Hasan, M.M. Masud, M.I. Nur Manik and M. Ahsan, *Asian J. Chem.*, **31**, 1842 (2019); https://doi.org/10.14233/ajchem.2019.21993
24. H. Tanaka, I. Atsumi, O. Shirota, S. Sekita, E. Sakai, M. Sato, J. Murata, H. Murata, D. Darnaedi and I.-S. Chen, *Chem. Biodivers.*, **8**, 476 (2011); https://doi.org/10.1002/cbdv.201000068

25. R. Haque, M.S. Ali, A. Saha and M. Alimuzzaman, *Dhaka Univ. J. Pharm. Sci.*, **5**, 77 (1970); https://doi.org/10.3329/dujps.v5i1.235
26. N. Santhiya, S. Priyanga, S. Hemmalakshmi and K. Devaki, *J. Appl. Pharm. Sci.*, **6**, 147 (2016); https://doi.org/10.7324/JAPS.2016.60722
27. M.M.N. Uddin, T.B. Emran, M. Mahib and R. Dash, *Bioinformation*, **10**, 630 (2014); https://doi.org/10.6026/97320630010630
28. G.K. Chatterjee, T.K. Burman, C.A. Nag and S.P. Pal, *Indian J. Pharm.*, **13**, 153 (1981).
29. J. Martins and S. Brijesh, *J. Ethnopharmacol.*, **248**, 112280 (2020); https://doi.org/10.1016/j.jep.2019.112280
30. S.K. Bhattacharya, P.K. Debnath, A.K. Sanyal and S. Ghoshal, *J. Res. Indian Med.*, **6**, 235 (1971).
31. V.S. Patil, H. Meena and D.R. Harish, *In Silico Pharmacol.*, **9**, 51 (2021); https://doi.org/10.1007/s40203-021-00110-0
32. H.B. Chu, Y.D. Tan, Y.J. Li, B.B. Cheng, B.Q. Rao and L.S. Zhou, *Afr. Health Sci.*, **19**, 2526 (2019); https://doi.org/10.4314/ahs.v19i3.28
33. P. Biradar, V. Patil, H. Joshi, P. Khanal and S. Mallapur, *Adv. Tradit. Med.*, **22**, 193 (2020); https://doi.org/10.1007/s13596-020-00524-9
34. P.H. Nguyen, T.N.A. Nguyen, T.T. Dao, H.W. Kang, D.T. Ndinteh, J.T. Mbafor and W.K. Oh, *J. Nat. Prod.*, **73**, 598 (2010); https://doi.org/10.1021/np900745g
35. H. Tanaka, M. Hirata, H. Etoh, M. Sako, M. Sato, J. Murata, H. Murata, D. Darnaedi and T. Fukai, *Chem. Biodivers.*, **1**, 1101 (2004); https://doi.org/10.1002/cbdv.200490082
36. D.C. To, T.Q. Bui, N.T.A. Nhung, Q.-T. Tran, T.-T. Do, M.-H. Tran, P.-P. Hien, T.-N. Ngu, P.-T. Quy, T.-H. Nguyen, H.-T. Nguyen, T.-D. Nguyen and P.-H. Nguyen, *Molecules*, **26**, 3691 (2021); https://doi.org/10.3390/molecules26123691
37. P.H. Nguyen, N.T.V. Trinh, T.T. Do, T.-H. Vu, D.C. To, H.K.T. Pham, P.C.H. Truong, K.T. Pham Van and M.H. Tran, *J. Chem. Res.*, **48**, 1 (2024); https://doi.org/10.1177/17475198231226382
38. H.M. Berman, J. Westbrook, Z. Feng, G. Gilliland, H. Weissig, T.N. Bhat, I.N. Shindyalov and P.E. Bourne, *Nucleic Acids Res.*, **28**, 235 (2000); https://doi.org/10.1093/nar/28.1.235
39. N. Guex and M.C. Peitsch, *Electrophoresis*, **18**, 2714 (1997); https://doi.org/10.1002/elps.1150181505
40. G.M. Morris, R. Huey, W. Lindstrom, M.F. Sanner, R.K. Belew, D.S. Goodsell and A.J. Olson, *J. Comput. Chem.*, **30**, 2785 (2009); https://doi.org/10.1002/jcc.21256
41. M.D. Hanwell, D.E. Curtis, D.C. Lonie, T. Vandermeersch, E. Zurek and G.R. Hutchison, *J. Cheminform.*, **4**, 17 (2012); https://doi.org/10.1186/1758-2946-4-17
42. O. Trott and A.J. Olson, *J. Comput. Chem.*, **31**, 455 (2010); https://doi.org/10.1002/jcc.21334
43. C.A. Lipinski, F. Lombardo, B.W. Dominy and P.J. Feeney, *Adv. Drug Deliv. Rev.*, **23**, 3 (1997); https://doi.org/10.1016/S0169-409X(96)00423-1
44. A. Daina, O. Michielin and V. Zoete, *Sci. Rep.*, **7**, 42717 (2017); https://doi.org/10.1038/srep42717
45. Y. Xu, J. Pei and L. Lai, *J. Chem. Inf. Model.*, **57**, 2672 (2017); https://doi.org/10.1021/acs.jcim.7b00244
46. J.P. Jang, M. Na, P.T. Thuong, D. Njamen, J.T. Mbafor, Z.T. Fomum, E.-R. Woo and W.K. Oh, *Chem. Pharm. Bull. (Tokyo)*, **56**, 85 (2008); https://doi.org/10.1248/cpb.56.85
47. C. Proença, M. Freitas, D. Ribeiro, E.F.T. Oliveira, J.L.C. Sousa, S.M. Tomé, M.J. Ramos, A.M.S. Silva, P.A. Fernandes and E. Fernandes, *J. Enzyme Inhib. Med. Chem.*, **32**, 1216 (2017); https://doi.org/10.1080/14756366.2017.1368503
48. B.J. Goldstein, *Curr. Drug Targets Immune Endocr. Metabol. Disord.*, **1**, 265 (2001); https://doi.org/10.2174/1568008013341163
49. C. Wiesmann, K.J. Barr, J. Kung, J. Zhu, D.A. Erlanson, W. Shen, B.J. Fahr, M. Zhong, L. Taylor, M. Randal, R.S. McDowell and S.K. Hansen, *Nat. Struct. Mol. Biol.*, **11**, 730 (2004); https://doi.org/10.1038/nsmb803
50. M.R. Groves, Z.J. Yao, P.P. Roller, T.R. Burke Jr. and D. Barford, *Biochemistry*, **37**, 17773 (1998); https://doi.org/10.1021/bi9816958